Electronic structure and Fermi-surface-related instabilities in $1T$-TaS_2 and $1T$-$TaSe_2$†

H. W. Myron
Department of Physics, Northwestern University, Evanston, Illinois 60201

A. J. Freeman
Department of Physics, Northwestern University, Evanston, Illinois 60201
and Argonne National Laboratory, Argonne, Illinois 60439
(Received 28 August 1974)

The electronic-energy-band structure and full-Brillouin-zone Fermi surfaces of the layered dichalcogenides, $1T$-TaS_2 and $1T$-$TaSe_2$, have been calculated using the Korringa-Kohn-Rostoker method in the muffin-tin approximation. We find that the Fermi surfaces for both systems away from symmetry points and lines have cross sections which are approximately constant along the z direction. Strong nesting features of the Fermi surface are found for a spanning vector parallel to the ΓM direction in reciprocal space with values in good agreement with the charge-density-wave results found by Wilson, Di Salvo, and Mahajan for these compounds.

I. INTRODUCTION

The two-dimensional nature of the bonding in the layered dichalcogenides is responsible for a number of their unusual physical properties. A variety of structural, electrical, magnetic, optical, and superconducting measurements have recently given a firm characterization of these properties. Most recently, the VB compounds of Ta and Nb have received a good deal of attention. In particular, the behavior of the resistivity in[1] $1T$-TaS_2 and[2] $1T$-$TaSe_2$ has been termed anomalous because the proposed band scheme of the $1T$ materials due to Wilson and Yoffe[3] predicts a partially filled high density of states d-band metal. This expected behavior is in keeping with the observation that in general the dichalcogenides formed from the group -IVB and -VIB transition-metal atoms exhibit semiconducting or insulating properties whereas the group-VB compounds tend to be metallic. $1T$-TaS_2 and $1T$-$TaSe_2$ are metallic above $T_d = 350$ K and $T_d = 473$ K, respectively, at which point there is a discontinuous change in the resistivity followed at lower temperatures by semiconductorlike behavior. The disulfide remains "semiconducting" below a second discontinuous bump in the resistivity which is centered around 190 K with a hysteresis 100 K wide.

Wilson *et al.*[2,4] have focused, in some detail, on the changes (structural, magnetic, optical, thermal etc.) which occur in these materials at a variety of first- and second-order transitions. They have associated this anomalous behavior with a nearly-two-dimensional Fermi surface supporting charge-density-wave (CDW) formation which in turn introduces a periodic lattice distortion (PLD) generally incommensurate with the lattice.[2,4] The amplitude of these incommensurate waves grows from a high temperature (below 550 K in $TaSe_2$) down as far as T_d, the first-order transition temperature which represents the point of conversion (or "lock-in") to a commensurate geometry.[4] Large, essentially parallel sections of Fermi surface were identified by Wilson *et al.*[2] from the argumented-plane-wave band calculations of Mattheiss[5] on $1T$-TaS_2 and generalized to interpret the electron diffraction and resistivity data observed for $1T$-$TaSe_2$.

In this paper we report results of detailed *ab initio* band-structure studies of the Fermi-surface (FS) geometry of $1T$-TaS_2 and $1T$-$TaSe_2$, which is believed to be responsible for the anomalous behavior of these compounds. From the calculated electronic band structure of both $1T$-TaS_2 and $1T$-$TaSe_2$, detailed full Brillouin-zone Fermi surfaces were constructed. We find that the FS's for both the disulfide and the diselenide are very similar, having FS cross sections in planar surfaces perpendicular to the layers which are approximately constant along the z direction and thus have large parallel sections which can be nested by approximately the same wave vector parallel to the ΓM direction. The theoretical resultant diffuse scattering wave vector for both $1T$-TaS_2 and $1T$-$TaSe_2$ is found to be in good agreement with the experimental values of Wilson *et al.*[4]

II. DETAILS OF THE CALCULATION AND ENERGY-BAND RESULTS

In the $1T$ polytype of the TaX_2 layered dichalcogenides, the chalcogen atoms are arranged about the tantalum atom on the corners of an octahedron. Each X-Ta-X sandwich is identical, and with each Ta lying over a Ta atom in the preceding sandwich there is just one per unit cell. For this crystal structure, the crystal potential was constructed along the usual lines[6] using the Hartree-Fock-Slater atomic charge densities from neutral atom configurations ($5d^4 6s^1$ on the tantalum atoms and p^4 on the anions), and full Slater ($\alpha = 1$) exchange.[7]

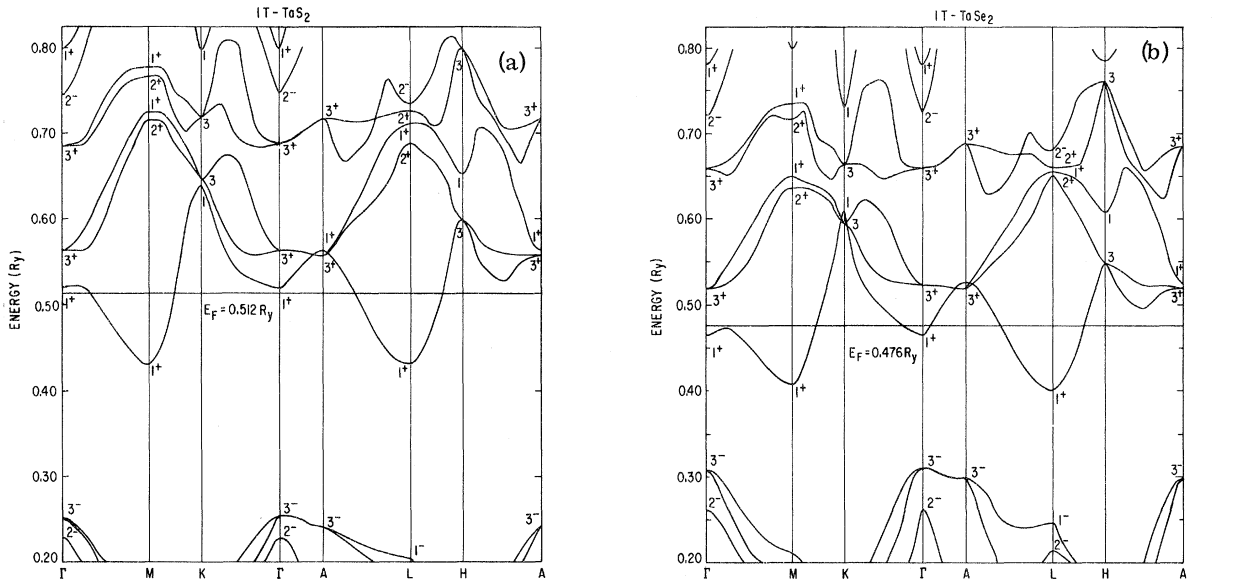

FIG. 1. (a) Ta-derived d bands of $1T$-TaS_2 and the top uppermost part of the S-derived p bands. (b) Ta-derived d bands of $1T$-$TaSe_2$ and the top uppermost part of the Se-derived p bands.

The muffin-tin radii (MT) were chosen in order to maximize the total electronic charge inside the MT spheres.[8] The lattice parameters are $a = 3.36$ Å, $c = 5.90$ Å,[9] and $a = 3.48$ Å, $c = 6.27$ Å,[10] respectively, for TaS_2 and $TaSe_2$; the MT radii for the Ta and anion spheres are, respectively, 2.118 and 2.476 a.u. for the case of TaS_2 and are 2.185 and 2.636 a.u. for the case of $TaSe_2$.

The energy bands have been calculated by the Korringa-Kohn-Rostoker[11] (KKR) method (in the muffin-tin approximation) for states up to $l = 2$ for both the metal and chalcogen atoms. The energy bands of the Ta derived d-like states of $1T$-TaS_2 and $1T$-$TaSe_2$ are plotted in Figs. 1(a) and 1(b), respectively, along the high-symmetry axes. (Also shown are the uppermost parts of the anion derived p bands and the p-d energy gap.)

The Fermi energies (E_F) of TaS_2 ($E_F = 0.512$ Ry) and $TaSe_2$ ($E_F = 0.476$ Ry) were found by fitting the calculated eigenvalues to a Fourier series and then sampling 13780 points in the irreducible zone in order to determine the integrated and the electronic density of states. The value of the density of states at E_F is 7.3 and 11.5 states/(Ry-atom-spin) for the disulfide and diselenide, respectively. The result for $N(E_F)$ of $1T$-TaS_2 is in relatively good agreement with a previous calculation of $N(E_F)$ which obtained a result of 6.7 states/(Ry atom spin).[5] The width of the occupied d conduction band obtained from photoemission studies on $1T$-TaS_2 (Ref. 12) is about 1.5 eV, in approximate agreement with the occupied-d-band width of Ref. 5 (1.15 eV) and the result of this work (1.19 eV). On the other hand, the calculated d-band width for $TaSe_2$ (0.9 eV) is in very good agreement with the width obtained from photoemission studies[13] (1.15 eV).

The results shown in Fig. 1 are consistent with the band structures of Murray and Yoffe[14] and certain changes in the measured optical properties[15] of these layered $1T$ systems when the sulfur atoms are replaced by the seleniums, namely: (i) the direct $p \rightarrow d$ band gap is reduced (from 0.265 Ry for $1T$-TaS_2 to 0.155 Ry for $1T$-$TaSe_2$); (ii) the so-called "hybridization" gap (the splitting between the t_{2g} and e_g states) is reduced[5]; (iii) the t_{2g}-band width is reduced[14,15]; (iv) the e_g-band width is increased.[14,15] These effects, which are gross features of the electronic structure of these materials, are evident even for the energy bands calculated with a MT potential.

Mattheiss's band calculation of $1T$-TaS_2,[5] which included the nonspherical contribution to the MT potential outside the MT spheres and utilized the augmented-plane-wave (APW) method, differs from the results of this calculation in the following important ways: there (i) the lowest 3^+ band and 1^+ at Γ are nearly degenerate; (ii) the hybridization gap between the lower and upper manifolds (of the d bands) is increased. However, the overall features of the band structure are the same; in particular, the lowest d band (which is half full) is topologically equivalent to the lowest band of this calculation. This determines the Fermi-surface

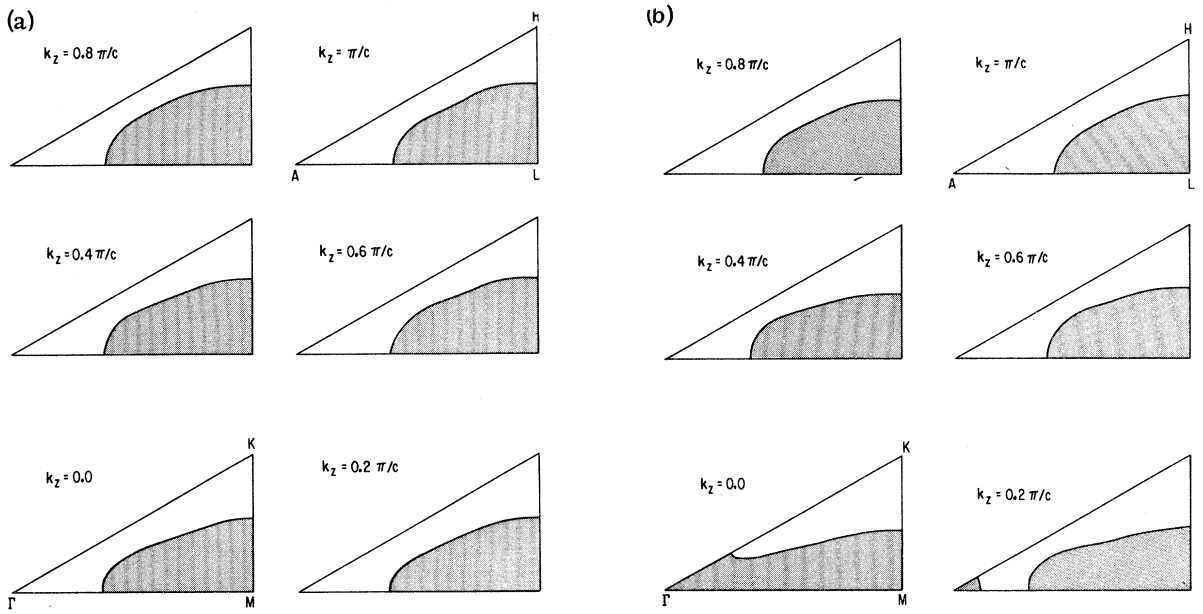

FIG. 2. (a) Fermi-surface cross sections of $1T$-TaS_2 along the k_z axis. (b) Fermi-surface cross sections of $1T$-$TaSe_2$ along the k_z axis.

geometry and nesting features. Since we are primarily concerned with the Fermi-surface geometry, a sufficiently large number of points in the irreducible Brillouin zone must be sampled; this becomes prohibitive in the APW calculation, where 160 basis functions are required in order to calculate an eigenvalue for a general point in the irreducible zone.[5] By contrast, the size of the secular determinant in our KKR calculations was 27, and included s, p, and d states of the metal and anions. The small size of the secular determinant enabled us to calculate eigenvalues on a sufficiently dense grid in the irreducible Brillouin zone to determine in detail the Fermi surface at many points in the zone.

III. FERMI-SURFACE-INDUCED INSTABILITIES

Since the work of Lomer[16] and Overhauser[17] it has been generally accepted that Fermi-surface nesting, i.e., the existence of large parallel pieces of Fermi surface, can lead to instabilities in the response of the conduction electrons. In a recent review, Chan and Heine[18] have explored the various possible instabilities caused by nesting situations. In one instability discussed by them, if the geometry is such that a vector $\vec{q}_0$ spans two nesting pieces of FS and the electron-phonon interaction is strong enough, then the phonon mode may become soft and a lattice distortion takes place that is generally incommensurate with the lattice. At present, neutron-diffraction studies are being performed[19] on the TaX_2 systems in order to verify whether the phonon mode becomes soft or whether a cusp is observed in the phonon spectra. As stated earlier, Wilson *et al.*[2,4] have also observed superlattice structure in their electron-diffraction studies which they related to lock in to the lattice of the hitherto incommensurate CDW.

Cross sections of the FS geometry determined from our KKR band calculations for the disulfide and the diselenide are shown in Figs. 2(a), and 2(b), respectively, along the k_z axis in increments of $0.2\pi/c$. Except for the additional section of the Fermi surface for the selenide in the vicinity of Γ (which may be the result of the use of the muffin-tin approximation) the geometries of the two systems are remarkably similar. For the TaS_2 and $TaSe_2$ cross sections, there is small variation in their dimensions as one proceeds along the k_z axis but in general the picture of the FS that emerges in the Brillouin zone (BZ) is one of essentially parallel flat walls in the vertical (k_z) direction. It thus appears likely that since a large electron-phonon interaction is present a lattice instability[18] will occur[2] in these materials.

To show the "nesting" features of the FS and how they relate to the CDW found experimentally, we plot in Fig. 3 the multiple sections of the FS in the basal plane of the hcp BZ and the extension of one segment outside the first zone. We note that the shape of the FS contour in the basal plane for TaS_2 lies between the contours shown by Wilson *et al.*[2,4] and by Williams *et al.*,[20] which were both derived from a limited number of k points given by Mattheiss in his calculation.[5] Our Fermi-sur-

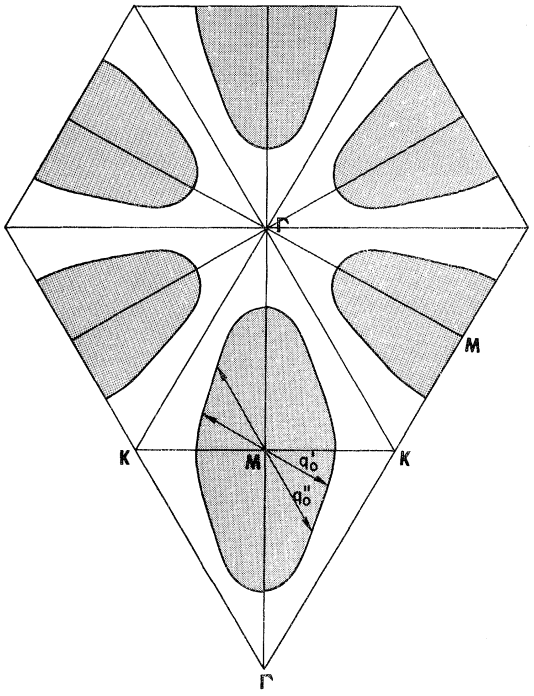

FIG. 3. Fermi-surface cross sections of $1T$-TaS_2 in the basal plane showing multiple segments and an extension of one segment into the next zone.

face contours were generated from 30 to 50 points in k space for each k_z plane shown (as opposed to the three points available from Mattheiss's work). The resultant rounded diamond shape has flat parallel sections between the minor and major axis which may be nested by spanning vectors such as the q_0' and q_0'' vectors shown in Fig. 3.

There is some small nesting across the single segment of our FS by a spanning vector, not shown in Fig. 3, in the MK direction (equivalent to the ΓK direction in the full zone) as originally selected by Wilson *et al.*[2] from their constructed Fermi surface to be responsible for the CDW. Large nesting will occur for a number of spanning vectors including both q_0' (parallel to ΓM) and q_0'' (parallel to ΓK) shown in Fig. 3. The most favorable single segment spanning vector is q_0' because this optimizes the nesting consistent with the rules[21] on Kohn anomalies minimizing the angle between the q vector and the electron velocity (which is normal to the FS) and because of the larger number of individual segments (four for ΓM vs two for ΓK) which will nest upon displacement by the spanning vectors along the directions in question[4] in the full k space. (This latter argument will not give rise to the spanning vector along ΓM for the alloying cases discussed below if one uses the Wilson *et al.* Fermi-surface sections.)

In their detailed report, Wilson *et al.*[4] show that the resultant CDW arises from a symmetry related set of the single segment FS spanning vectors, q_0', which are parallel to ΓM. Expressed in units of $a_0^* = 4\pi/\sqrt{3}a_0$ our averaged q_0' values, equal to 0.34 for TaS_2 and 0.32 for $TaSe_2$, are in good agreement with the values, 0.288 ± 0.005 and 0.285 ± 0.005, respectively, obtained by Wilson *et al.*[4] for the CDW in the incommensurate state. At lock-in they find $q_0'/a_0^* = 1/\sqrt{13}$ for $1T$-$TaSe_2$ and almost this value for $1T$-TaS_2.

Finally, Wilson *et al.*[4] also found that the temperature T_d, at which the $\sqrt{13}\,a_0$ superlattice is

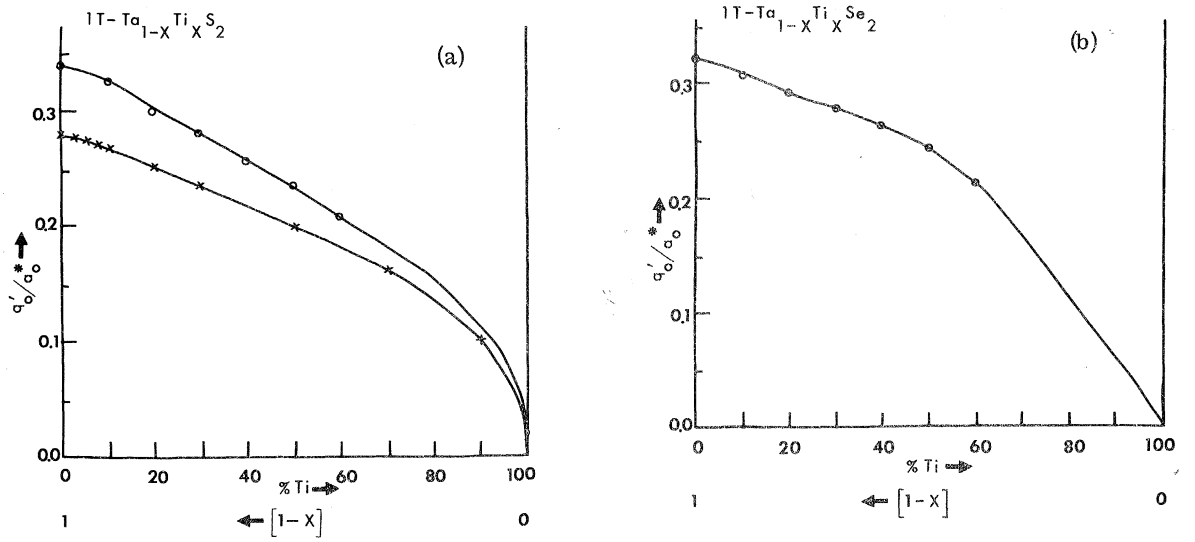

FIG. 4. (a) Rigid-band estimates of q_0'/a_0^* vs electron content for $1T$-$Ta_{1-x}Ti_xS_2$. The line drawn through the crosses is the result of Wilson *et al.* (Ref. 4). (b) Rigid-band estimates of q_0'/a_0^* vs electron content for $1T$-$Ta_{1-x}Ti_xSe_2$.

adopted is quite strongly affected by substitutional doping and that the prime factor in reducing T_d is disorder and not the change in the average electron content, electrons per atom. They determined the diffuse scattering vector as a function of Ti concentration in $Ta_xTi_{1-x}S_2$ in order to demonstrate that the scattering is related to the FS geometry. Using a rigid band model and Mattheiss's energy bands for $1T$-TaS_2, they showed that q_0'/a_0^* followed a parabolic (x^2) dependence on concentration of Ti in $1T$-$Ta_xTi_{1-x}S_2$ for small x, as expected from the parabolic shape of the bands at their lowest energies. Estimates of the behavior of q_0'/a_0^* vs x for the Ta-rich alloys may be made using our detailed energy-band and density-of-states results. If we assume a rigid-band model, no lattice contraction upon Ti doping and use our density-of-states results to determine, at each Ti concentration, the E_F and the Fermi-surface cross sections we can, for both $Ta_xTi_{1-x}S_2$ and $Ta_xTi_{1-x}Se_2$, determine theoretically the corresponding q_0' spanning vectors values. These results are shown in Figs. 4(a) and 4(b); comparison with the Wilson *et al.*[4] values for $Ta_xTi_{1-x}S_2$, also shown in Fig. 4(a) shows surprisingly good agreement between these crude theoretical estimates and experiment.

IV. CONCLUSION

We have found that *ab initio* KKR energy-band calculations yield Fermi surfaces which are in good agreement with experiment. The *flat* parallel sections of the FS in planes perpendicular to the z axis of the zone give large FS nesting features and spanning vectors which have approximately the magnitudes found by Wilson *et al.*[2,4] and lie along the ΓM direction as found for the CDW's in these systems. These results give strong confirmation to the view that FS nesting features give rise, through instabilities in the response of the conduction electrons and the existence of large electron-phonon interactions, to the observed CDW's. Calculations are now in progress to relate more closely the Fermi-surface nesting features to maxima in the generalized susceptibility $\chi(q)$ and experiment.[19]

ACKNOWLEDGMENTS

We are indebted to J. R. Revelli and D. E. Ellis for informative discussions and one of us (H.W.M.) is indebted to J. A. Wilson for an early discussion of his work.

---

†Work supported by the Air Force Office of Scientific Research, the National Science Foundation through Northwestern University Materials Research Center, and the U. S. Atomic Energy Commission.

[1]A. H. Thompson, F. R. Gamble, and J. R. Revelli, Solid State Commun. 9, 981 (1971).
[2]J. A. Wilson, F. J. DiSalvo, and S. Mahajan, Phys. Rev. Lett. 32, 882 (1974).
[3]J. A. Wilson and A. D. Yoffe, Adv. Phys. 18, 193 (1969).
[4]J. A. Wilson, F. J. DiSalvo, and S. Mahajan, Adv. Phys. (to be published).
[5]L. F. Mattheiss, Phys. Rev. B 8, 3719 (1973).
[6]L. F. Mattheiss, Phys. Rev. 133, A1399 (1964).
[7]J. C. Slater, Phys. Rev. 81, 385 (1951).
[8]A. J. Freeman and D. D. Koelling, J. Phys. 33, C3-57 (1972).
[9]A. H. Thompson, K. R. Pisharody, and R. F. Koehler, Jr., Phys. Rev. Lett. 29, 163 (1972).
[10]F. J. DiSalvo, R. G. Maines, J. R. Waszczak, and R. E. Schwall, Solid State Commun. 14, 497 (1974).
[11]J. Korringa, Physica 13, 392 (1947); W. Kohn and N. Rostoker, Phys. Rev. 94, 1111 (1954).
[12]P. M. Williams and F. R. Shepherd, J. Phys. C 5, L36 (1973).
[13]M. M. Traum, N. V. Smith, and F. J. DiSalvo, Phys. Rev. Lett. 32, 1241 (1974).
[14]R. B. Murray and A. D. Yoffee, J. Phys. C 5, 3038 (1972).
[15]A. R. Beal, J. C. Knight, and W. Y. Liang, J. Phys. C 5, 3531 (1972).
[16]W. M. Lomer, Proc. Phys. Soc. Lond. 80, 489 (1962).
[17]A. W. Overhauser, Phys. Rev. 167, 691 (1968); B 3, 3173 (1971).
[18]S-K Chan and V. Heine, J. Phys. F 3, 795 (1973).
[19]D. E. Moncton and J. D. Axe (unpublished results).
[20]P. N. Williams, G. S. Parry, and C. B. Scruby, Philos. Mag. 29, 695 (1974).
[21]See discussion by C. B. Walker and P. A. Egelstaff [Phys. Rev. 177, 1111 (1969), and references therein].